0026-895X/93/040635-10$03.00/0

MOLECULAR PHARMACOLOGY, 43:635-644

Site-Directed Mutagenesis of the Putative Pore Region of the Rat IIA Sodium Channel

KRIS J. KONTIS and ALAN L. GOLDIN

Department of Microbiology and Molecular Genetics, University of California, Irvine, California 92717

Received December 4, 1992; Accepted January 24, 1993

SUMMARY

We have used site-directed mutagenesis to examine the functional role of each of the eight acidic amino acid residues in the region between proposed transmembrane segments 5 and 6 (S5-S6) of domain II of the rat brain IIA sodium channel α subunit. The mutant sodium channels were expressed in *Xenopus* oocytes and analyzed by two-microelectrode voltage clamping with respect to voltage-dependent activation, inactivation, ion selectivity, and sensitivity to the pore-blocking neurotoxins tetrodotoxin (TTX) and saxitoxin (STX). None of the mutations had significant effects on voltage-dependent gating, ion selectivity, or block by protons or calcium. Three of the mutations had significant effects on the sensitivity of the channel to block by TTX and STX. Neutralization of negative charges at positions 942 and 945 greatly reduced the block by TTX and STX, suggesting that these two residues interact directly with the toxins. Substitution of a nearby negative charge at position 949 resulted in a smaller decrease in TTX and STX block, although analysis of TTX block of this mutant at low ionic strength suggests that the interaction is not simply by an electrostatic through-space mechanism. None of the other five mutations had any effects on block by either TTX or STX. The two acidic residues that had dramatic effects on toxin binding had significantly smaller effects at a depolarized membrane potential. The sodium channel interacts with TTX and STX with higher affinity at depolarized potentials, so these two residues must make a greater contribution to toxin binding in the low affinity state. These results define a small segment of the sodium channel α subunit domain II S5-S6 region that interacts with TTX and STX and therefore must lie near the mouth of the channel pore.

Voltage-gated sodium channels mediate the rapid membrane depolarization during generation of action potentials in most excitable cells. The channels are characterized by voltage-dependent activation, rapid inactivation, and high selectivity for sodium ions over other monovalent cations. One of the most powerful approaches used to investigate sodium channel structure/function has been the combination of molecular biology techniques and the use of specific neurotoxin probes. The guanidinium toxins TTX and STX are specific blockers of sodium channels (1). Current models of TTX block propose that the positively charged toxin molecule binds at the external mouth of the pore, preventing conduction of sodium ions by acting like a "lid" (2). Although block by TTX was originally thought to be independent of channel gating (1), more recent evidence has indicated that sodium channels from cardiac muscle (3–5), denervated skeletal muscle (6), crayfish giant axon (7), frog myelinated axon (8), and rat brain (9) are all blocked by TTX in a use-dependent fashion.

Sodium channels are members of a large family of structurally related cation-selective channels, including potassium channels and calcium channels. Studies on potassium channels have provided insights into the basis for sensitivity to pore-blocking agents and ion selectivity. Amino acid residues in the region between proposed transmembrane segments S5 and S6 (the S5-S6 segment) of *Shaker* B potassium channels have been shown to be involved in the binding of charybdotoxin and TEA ion, two reagents that are known to block potassium channels by binding near the mouth of the pore (10, 11). Some mutations in this region affect internal TEA binding, whereas others affect only external TEA binding (12, 13). Hartmann *et al.* (14) have shown that both the single-channel conductance and the TEA sensitivity of NGK2 K^+ channels can be transferred to DRK1 K^+ channels by exchanging only the S5-S6 segment. Finally, mutations within this region in *Shaker* A channels have been shown to increase the permeability to rubidium and ammonium ions (15). All of these data indicate that the S5-S6 segment lines the actual pore of the channel. Models consistent with the data portray this segment as a short loop spanning the membrane of the cell (16, 17).

The S5-S6 regions of rat brain sodium channels have also been shown to be important for toxin binding and sodium conductance. Noda *et al.* (18) have shown that TTX and STX

This research was supported by grants from the United States National Institutes of Health (NS-26729) and the Lucille P. Markey Charitable Trust. K.J.K. was supported by a postdoctoral fellowship from the National Multiple Sclerosis Society (FG 835-A-1). A.L.G. is a Lucille P. Markey Scholar.

ABBREVIATIONS: TTX, tetrodotoxin; STX, saxitoxin; TEA, tetraethylammonium; HEPES, 4-(2-hydroxyethyl)-1-piperazineethanesulfonic acid.

sensitivity of the rat brain type II sodium channel is greatly reduced by neutralization of the negative glutamate at position 387 in the S5-S6 region of domain I. Terlau *et al.* (19) made substitutions at the analogous amino acid positions in all four domains of the rat type II channel (positions 384 and 387 in domain I, 942 and 945 in domain II, 1422 and 1425 in domain III, and 1714 and 1717 in domain IV). Six of these sites (positions 384, 387, 942, 945, 1425, and 1717) normally contain negative charges in the sodium channel, and neutralization of any of these sites results in resistance to TTX and STX and decreased sodium conductance. The two sites that do not normally contain negative charges are lysine at position 1422 and alanine at position 1714. Heinemann *et al.* (20) have shown that mutation of either of these residues to a negatively charged glutamate results in a channel with selectivity properties similar to those of voltage-dependent calcium channels. All of these results indicate that the four domains of the sodium channel contain major determinants of TTX and STX binding and that domains III and IV contain residues important for calcium permeability.

In this paper we have quantitatively evaluated the importance of each of the acidic residues in the S5-S6 region of one representative domain of the sodium channel. Previous studies have shown that acidic residues are important in determining some of the characteristics of sodium channel function. Treatment with carboxyl-modifying reagents is known to reduce susceptibility to TTX block and to cause a reduction in single-channel conductance (21). In addition, the binding site for proton block is thought to consist of one or more carboxylic acid side chains (22). To more completely evaluate the importance of the acidic residues in the S5-S6 region for sodium ion permeation, we constructed mutations neutralizing each of the eight acidic residues in this region of domain II of the rat brain type IIA sodium channel. The mutant channels were then analyzed with respect to the properties of voltage-dependent activation and inactivation, block by TTX and STX, selectivity, and calcium and proton block.

Materials and Methods

Construction of sodium channel mutations. The plasmid pVA2580 contains the wild-type rat IIA sodium channel α subunit following a T7 RNA polymerase promoter (23). The *Sph*I-*Bgl*II fragment from this plasmid, containing the domain II S5-S6 region, was subcloned into an m13 phage with a custom polylinker. Uracil-containing single-stranded DNA was synthesized by growth in the *dut*$^-$, *ung*$^-$ *Escherichia coli* strain RZ1032 (24). For site-directed mutagenesis, kinased oligonucleotide primers were annealed to the template at a 10:1 molar ratio. The primers were extended with T4 DNA polymerase (2.5 units) in the presence of T4 DNA ligase (6 Weiss units), in a 100-μl reaction containing 100 mM Tris·HCl, pH 7.5, 50 mM $MgCl_2$, 2.5 mM dATP, 2.5 mM dCTP, 2.5 mM dGTP, 2.5 mM TTP, 2.5 mM ATP, and 1 mM dithiothreitol. The reactions were incubated on ice for 5 min, at 22–26° for 5 min, and then at 37° for 2 hr. Reaction products were precipitated with ethanol and resuspended in 20 μl of H_2O. *E. coli* strain XL-1 (*ung*$^+$) was electroporated using 1 μl of the synthesis reaction, and plaques were picked and used to generate single-stranded DNA, which was then screened by dideoxynucleotide sequencing to confirm mutations. The *Sph*I-*Bgl*II fragments containing the mutations were then ligated into the full-length cDNA clone pVA2580, which was confirmed by sequencing. The constructs were named according to the resulting amino acid substitution (using the standard one-letter amino acid abbreviations).

Expression of sodium channel mRNA in *Xenopus* oocytes. Plasmid DNA containing the full-length sodium channel coding region was linearized by digestion with *Cla*I and 5 μg were used for *in vitro* transcription in 100-μl reactions containing 200 units of T7 RNA polymerase (New England Biolabs), as described previously (23). Transcription reactions were incubated for 3 hr at 37°, and the transcripts were purified on spun columns containing Sephacryl S-400, precipitated with ethanol twice, and dissolved in 1 mM Tris·HCl, pH 6.5, for injection. Stage V oocytes were obtained from adult female *Xenopus laevis* frogs (Xenopus I), defolliculated with collagenase, and injected with 0.2–14 ng of *in vitro* transcribed RNA. The amount of RNA injected for each construct was chosen to result in current amplitudes of 1–2 μA. The oocytes were incubated for 2 days at 20° in ND96 (see below) containing 550 mg/liter sodium pyruvate, 0.5 mM theophylline, and 50 μg/ml gentamicin.

Electrophysiological recording. Sodium currents were measured by two-electrode voltage clamping as described previously (25). Borosilicate glass electrodes were filled with filtered 3 M KCl and had impedances between 0.5 and 1 MΩ, and currents were measured using a virtual ground circuit. Oocytes were clamped at a holding potential of −100 mV for at least 5 min before recording to ensure a steady state level of current. The standard recording bath solution contained 96 mM NaCl, 2 mM KCl, 1 mM $MgCl_2$, 1.8 mM $CaCl_2$, and 5 mM HEPES, pH 7.5 (ND96). Low pH recordings used ND96 with a final pH of 6.0, and low calcium recordings used ND96 containing 0.18 mM $CaCl_2$ instead of 1.8 mM. Additional bath solutions contained 96 mM guanidine-HCl or 96 mM LiCl instead of NaCl but were otherwise identical to ND96. TTX and STX (Calbiochem) were added from 1 mM stock solutions and mixed with the standard recording bath solution. All experiments were performed at room temperature (20–22°). Capacitive transient and linear leak currents were corrected by a P/4 protocol or by subtraction of records obtained in the presence of 1 mM TTX (for TTX-sensitive channels). Series resistance varied from 1 to 2.5 kΩ.

Data analysis. Electrophysiological data were obtained and analyzed using the pCLAMP programs (version 5.5.1; Axon Instruments, Burlingame, CA) (26). Data were filtered on-line using an eight-pole Bessel filter and were then digitized at a sampling frequency of 12.5 kHz. Nonlinear curve-fitting was done using the Sigmaplot program (version 4.0; Jandel Scientific), which uses the Marquardt-Levenberg algorithm for nonlinear regression. Conductance values (G) were calculated by measuring the peak current at test potentials from −90 to +55 mV and dividing by $(V - V_{rev})$, where V is the test potential and V_{rev} is the reversal potential. Reversal potentials were individually estimated for each data set by least squares fit of I-V data to a Boltzmann function of the form

$$G = \frac{1}{1 + \exp[-0.03937 \cdot z \cdot (V - V_{1/2})]} \cdot g \cdot (V - V_{rev})$$

where z is the apparent gating charge, g is a factor related to the number of channels contributing to the macroscopic current, V is the potential of the voltage pulse, and $V_{1/2}$ is the half-maximal voltage. Peak conductance-voltage relationships were fit with a two-state Boltzmann function,

$$G = \frac{1}{1 + \exp[-0.03937 \cdot z \cdot (V - V_{1/2})]}$$

Inactivation data were acquired using a two-pulse protocol consisting of either 50-msec or 10-sec prepulses ranging from −95 to +15 mV, followed by 12-msec test pulses to −5 mV to measure the availability of channel openings. Two-pulse inactivation data were fitted with a two-state Boltzmann function,

$$I = \frac{1}{1 + \exp[(V - V_{1/2})/a]}$$

where a is the slope factor and $V_{1/2}$ is the voltage for half-maximal inactivation.

Dose-response curves for TTX and STX block were determined by measurement of peak currents while the oocytes were being perfused with standard bath recording solution, followed by measurement of peak currents after addition of either TTX or STX to the bath. Test pulses were given 60–90 sec apart to avoid artifacts due to use dependence, and currents were measured after a steady state block was obtained (usually within 5 min). The TTX- or STX-containing bath solution was then washed out with 10 bath volumes of standard bath solution and the peak currents were again measured to assess current run-down. Dose-response data were fitted using the Langmuir adsorption isotherm,

$$F_c = [1 + (T/K_{app})^n]^{-1},$$

where F_c is the fraction of maximal current remaining after block by TTX or STX, T is the toxin concentration, K_{app} is the concentration of toxin at half-maximal block, and n is the Hill coefficient.

pK_a values were estimated by fitting normalized conductances to the following model (22):

$$\frac{G}{G_{max}} = \frac{1}{1 + \exp[-0.03937 \cdot z \cdot (V - V_{1/2})]} \cdot \frac{K_a \cdot \exp[n \cdot \delta \cdot V \cdot (0.03937)]}{[H^+]_0 + K_a \cdot \exp[n \cdot \delta \cdot V \cdot (0.03937)]}$$

where n is the valence of the blocking ion, δ is the fraction of the membrane electric field (assumed to be 0.24), and K_a is the dissociation constant.

Results

Voltage-dependent gating properties of sodium channels with mutations in domain II S5-S6. The sodium channel α subunit consists of four homologous domains termed I-IV. Each of these domains contains an S5-S6 region, which contains many acidic residues and is thought to form part of the pore-forming region of the channel. To test the importance of each of the acidic residues in sodium ion permeation we have chosen to concentrate on one domain (II). As shown in Fig. 1, the domain II S5-S6 region contains eight negatively charged aspartate or glutamate residues. We have individually neutralized each of these charges by changing the aspartates to asparagines and the glutamates to glutamines. Before testing the permeation properties of these mutants, however, we first wanted to determine whether any of the mutations affected the voltage-dependent properties of the channel. We therefore expressed each of the mutants in *Xenopus* oocytes and examined the voltage dependence of peak conductance and inactivation by two-microelectrode voltage clamping. Representative current traces for the wild-type sodium channel are shown in Fig. 2A. All of the mutants had kinetics of inactivation comparable to those of the wild-type channel, and the levels of peak sodium current were also comparable for all of the mutants except E942Q. Peak currents for this mutant were about 10-fold smaller than for the wild-type channel after injection of the same amount of RNA. The voltage dependence of peak conductance for all of the mutants was not significantly different from that of the wild-type channel (Fig. 2B; Table 1). With respect to inactivation, we examined voltage dependence using a two-pulse protocol with either a short (50-msec; Fig. 2C) or a long (10-sec; Fig. 2D) inactivating prepulse. As with peak conductance, none of the mutants were significantly different from the wild-type channel (see also Table 1). These results indicate that none of the negative charges in the domain II S5-S6 region have a significant role in voltage-dependent gating of the channel.

TTX and STX sensitivity of the mutants. We next wanted to determine whether any of these acidic residues were involved in inhibition of the channel by TTX or STX. As shown in Fig. 3A and Table 2, three of the mutants were significantly more resistant to block by TTX than was the wild-type channel. The wild-type channel was inhibited by TTX with a K_{app} of 18.6 nM. Two of the mutants were highly resistant to TTX, with a K_{app} of 32.7 μM for mutant E942Q and a K_{app} of 5.4 μM for mutant E945Q. The third mutant, D949N, was only slightly more resistant than the wild-type channel, with a K_{app} of 46 nM. Similar results were observed with respect to block by STX, with the same three mutants being resistant to the toxin (Fig. 3B). The wild-type channel was blocked by STX with a K_{app} of 2.8 nM, whereas E942Q had a K_{app} of 4.8 μM and E945Q had a K_{app} of 54 μM. Mutant D949N was again only slightly more resistant to STX than was the wild-type channel, with a K_{app} of 8.8 nM. The other five mutants were all as sensitive to block by both TTX and STX as was the wild-type channel (Table 2). In all cases the dose-response curves indicated Hill coefficients that reflected a one-to-one stoichiometry for block by both toxins. Interestingly, E942Q was more resistant to TTX than to STX, and E945Q was more resistant to STX than to TTX. The results for these two mutants are consistent with the findings of Terlau *et al.* (19).

TTX sensitivity at low ionic strength. The slight effect that the D949N mutation had on TTX binding suggested that

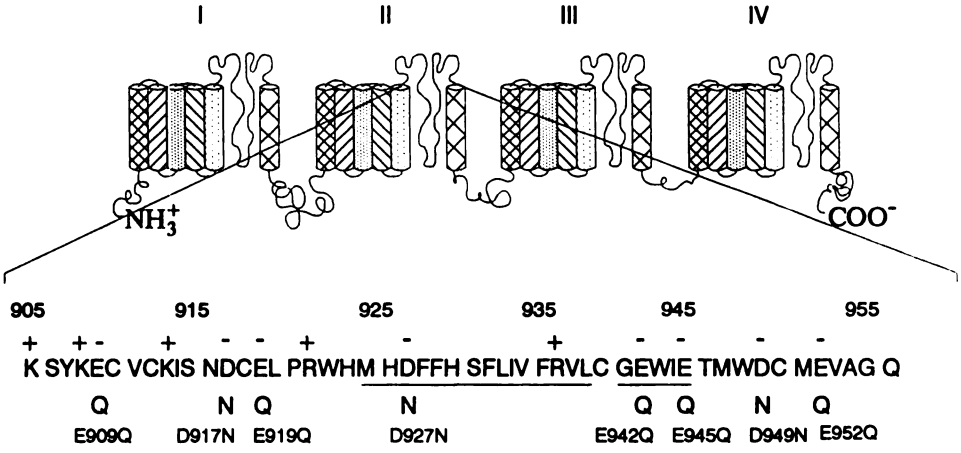

Fig. 1. Diagram of mutations. The amino acid sequence between putative transmembrane segments S5 and S6 in domain II of the rat brain IIA sodium channel α subunit is shown. The single-amino acid substitution mutations used in this study are shown *below the sequence*. The *underlined* regions represent the putative pore-spanning regions of the channel (SS1 and SS2) (16).

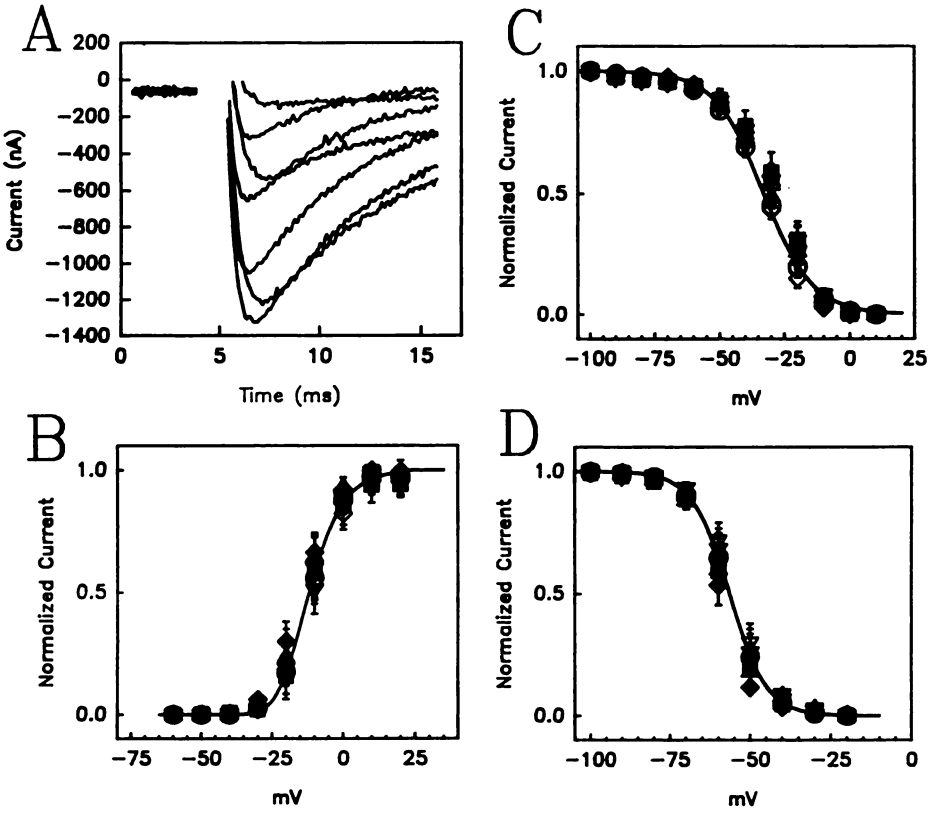

Fig. 2. Voltage-dependent gating properties of wild-type and mutant sodium channels. A, Oocytes injected with RNA encoding the wild-type sodium channel were held at −100 mV, and sodium currents were elicited with 12-msec test pulses from −90 to +55 mV in 5-mV increments. Current traces are shown during depolarizations from −30 mV to +30 mV in 10-mV increments. B, Voltage dependence of peak conductance of wild-type sodium channels is compared with that of all eight mutants. Sodium currents were recorded as in A, and conductance values for depolarization to every 10 mV are shown. Peak currents were converted to conductances as described in Materials and Methods. C and D, Voltage dependence of inactivation was determined by a two-pulse protocol in which oocytes were held at −100 mV and depolarized from −90 to +15 mV for 50 msec (C) or 10 sec (D), followed by a 12-msec test pulse to 0 mV to determine the available current. The *data points* in B, C, and D represent at least three determinations and the *error bars* are 1 SD. The *smooth curves* were derived from fitting the wild-type data with a two-state Boltzmann function, as described in Materials and Methods. Although the individual symbols cannot be clearly distinguished, they represent wild-type (○), E909Q (▽), D917N (□), E919Q (△), D927N (◇), E942Q (◆), E945Q (▲), D949N (■), and E952Q (▼).

TABLE 1

Macroscopic activation and inactivation parameters of wild-type and mutant sodium channels

Data were fit to two-state Boltzmann functions as described in Materials and Methods. Z_{app} is the apparent gating charge, $V_{½}$ is the voltage of half-maximal current, and *a* is the slope factor.

	G-V		50-msec prepulse		10-sec prepulse	
	Z_{app} (e_0)	$V_{½}$	*a*	$V_{½}$	*a*	$V_{½}$
		mV	mV	mV	mV	mV
Wild-type	4.5 ± 0.2	−11.3 ± 1.7	9.6 ± 1.3	−33.0 ± 1.8	5.7 ± 0.6	−56.5 ± 2.2
E909Q	4.7 ± 0.1	−10.3 ± 0.8	9.3 ± 0.3	−29.5 ± 3.5	6.0 ± 0.3	−54.6 ± 1.5
D917N	4.9 ± 0.5	−11.0 ± 1.6	8.3 ± 0.5	−33.0 ± 1.7	5.8 ± 0.1	−57.4 ± 2.1
E919Q	4.6 ± 0.2	−12.0 ± 3.5	9.5 ± 0.7	−31.4 ± 0.1	5.7 ± 0.2	−57.8 ± 1.6
D927N	4.1 ± 0.5	−10.4 ± 1.0	10.2 ± 0.7	−29.5 ± 2.8	5.7 ± 0.5	−56.5 ± 1.8
E942Q	4.3 ± 0	−14.5 ± 2.0	8.9 ± 0.8	−28.3 ± 3.2	5.0 ± 0.4	−59.5 ± 1.5
E945Q	4.8 ± 0.2	−13.5 ± 1.7	9.2 ± 0.5	−29.9 ± 2.3	6.1 ± 0.3	−55.9 ± 2.2
D949N	4.4 ± 0.3	−11.7 ± 2.5	9.0 ± 0.4	−28.9 ± 1.7	5.7 ± 0.2	−57.8 ± 2.0
E952Q	4.3 ± 0.7	−11.5 ± 2.8	8.7 ± 0.3	−29.4 ± 4.2	5.5 ± 0.7	−55.5 ± 3.0

the aspartate at position 949 might be interacting with TTX electrostatically through space. If this were the case, then decreasing the ionic strength of the extracellular environment would have a lesser effect on the TTX binding of the mutant than on that of the wild-type channel. We therefore measured the TTX sensitivity of the wild-type channel and the D949N mutant channel in medium containing half the normal concentration of sodium (48 mM instead of 96 mM). As shown in Fig. 4A, the wild-type channel was blocked with a K_{app} of 11.5 ± 0.9 nM and D949N was blocked with a K_{app} of 27.3 ± 3.0 nM. Fig. 4B shows that the decreases in the K_{app} values at low ionic strength are similar for the wild-type channel and D949N. Therefore, the contribution to TTX binding made by D949 does not appear to be affected by ionic strength, suggesting that the interaction is not simply electrostatic through space.

TTX sensitivity at the depolarized holding potential of −60 mV. Patton and Goldin (9) showed that rat IIA sodium channels expressed in *Xenopus* oocytes are blocked by TTX in a use-dependent manner. The use dependence most likely reflects an increased affinity of the channels for TTX at depolarized potentials. Consistent with this change in affinity, the K_{app} was 18 nM at a holding potential of −100 mV, whereas the K_{app} was reduced to 7 nM at the relatively depolarized holding potential of −60 mV. To test whether the negatively charged residues in the domain II S5-S6 region were involved in TTX binding in the high affinity state, we measured the K_{app} at a holding potential of −60 mV. All of the mutants had increased affinities for TTX at −60 mV, compared with −100 mV (Table 3). The ratio of K_{app} at −100 mV to K_{app} at −60 mV for the wild-type channel was 2.7, and the ratios for the five mutants that were as sensitive to block by TTX as was the wild-type channel ranged from 1.9 to 3.3. Mutant D949N, which was

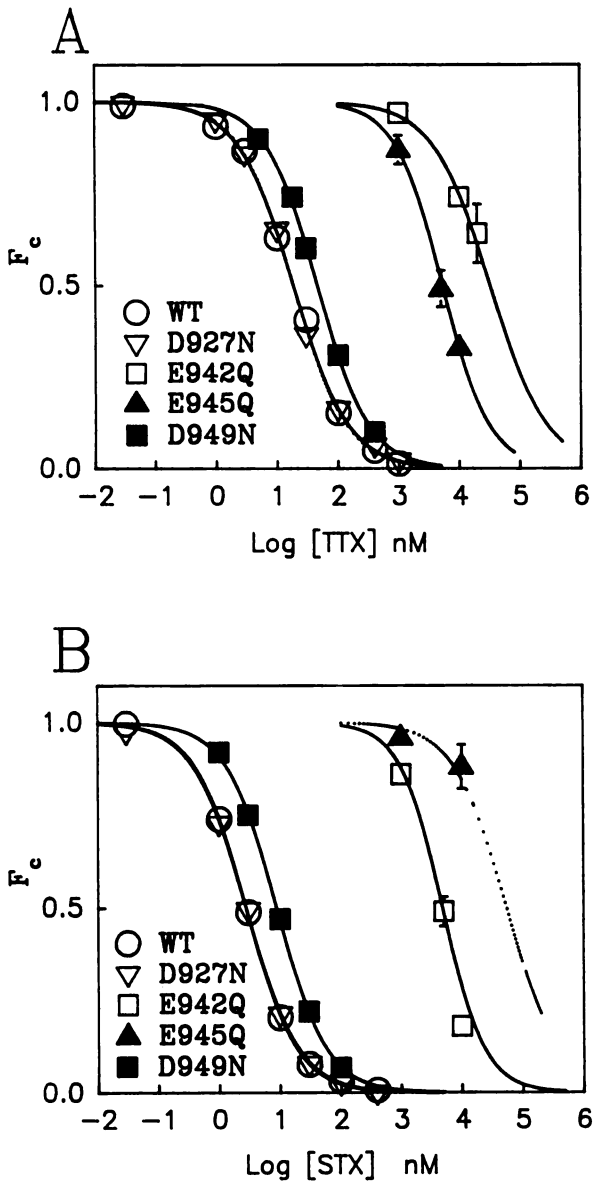

Fig. 3. TTX and STX dose-response curves. Oocytes expressing wild-type (*WT*) or mutant sodium channels were perfused with ND96 and peak sodium currents were measured at test potentials known to elicit the maximum inward current (between 0 and −5 mV). Peak currents were again measured after perfusion of the recording chamber with at least 10 bath volumes of ND96 containing varying concentrations of TTX (A) or STX (B). To avoid use-dependent block, pulses were no more frequent than 90 sec apart. The oocytes were then perfused with ND96 to allow measurement of the peak current after the toxins had been washed out. *Data points* represent the means of at least three separate determinations, and the *error bars* are standard deviations. The *curves* were generated by a best fit to a Langmuir isotherm as described in Materials and Methods.

slightly more resistant to block by TTX than was the wild-type channel, similarly displayed a 2.5-fold increase in affinity at −60 mV. The two mutants that were highly resistant to TTX (E942Q and E945Q) were more sensitive to block by TTX at −60 mV, but with ratios of 9.9 and 11.3. These results indicate that all of the mutant channels were more sensitive to block by TTX at depolarized holding potentials, similar to the wild-type channel. However, the two mutations that dramatically affected toxin sensitivity at −100 mV did not alter it quite as much at −60 mV.

Relative permeability of guanidinium and lithium ions. TTX is known to block sodium channels by binding near the external mouth of the pore (2). Because three of the negative charge mutations affected the TTX sensitivity of the channel, it was possible that these mutations may have also affected selectivity. To determine whether this was the case, we examined the reversal potentials of the wild-type and mutant channels in the presence of sodium, guanidinium, and lithium. The permeability to guanidinium of sodium channels in frog myelinated axons has been shown to be 0.13, relative to sodium. We measured reversal potentials using an external solution containing 96 mM guanidinium instead of sodium. Under these conditions the inward currents were much smaller than those observed with an external solution of 96 mM sodium, and it was not possible to measure the guanidinium and sodium reversal potentials in the same oocyte. Fig. 5A shows representative current traces from an oocyte that expressed the wild-type sodium channel and was bathed with 96 mM guanidinium. The inward sodium current was >50 μA when an external solution containing 96 mM sodium was used (data not shown). The current-voltage relationship shows that the outward currents increased in a linear fashion, with an apparent reversal potential of about 9 mV (Fig. 5B). The average reversal potential of the wild-type sodium channel in the presence of 96 mM external guanidinium was 12 mV, as shown in Fig. 5C. The mutant channels had reversal potentials that ranged from 8 to 16 mV (Fig. 5C). None of these values was significantly different from that for the wild-type channel, and in fact the variation is most likely due to differences in the internal concentrations of permeant ions in oocytes from different frogs. These results suggest that permeability to guanidinium is not significantly affected by these mutations.

We also estimated the relative permeabilities of the mutant channels to lithium, compared with sodium. The relative permeability of wild-type sodium channels to lithium has been shown to be about 1.0 (27, 28). The Goldman-Hodgkin-Katz equation allows the estimation of relative permeabilities based on reversal potentials measured in the presence of different permeant ions in the external bath. Based on reversal potentials, all of the mutants had permeability ratios similar to that of the wild-type channel (data not shown). However, Hille (29) has observed that lithium currents in myelinated nerve are typically smaller than would be predicted by the independence principle. He suggested that this might be caused by lithium ions taking a long time to pass through or dissociate from the channel, thus delaying passage of other ions. We tested whether lithium ions also decrease currents through the wild-type and mutant channels expressed in *Xenopus* oocytes. The wild-type sodium channel was blocked by lithium ions, as shown in Fig. 6. The ratio of peak current in the presence of 96 mM external lithium to that in the presence of 96 mM external sodium averaged 0.75 (Table 4). All of the mutant sodium channels were blocked by lithium to about the same extent, with the ratio of currents ranging from 0.76 to 0.86 (Table 4). These data suggest that none of the negatively charged residues in the domain II S5-S6 region is critical for determining selectivity of the channel for sodium, compared with lithium and guanidinium.

Block of mutant sodium channels by protons and calcium. It has previously been shown that sodium channels are blocked by calcium ions in a voltage-dependent manner (22,

TABLE 2

Parameters of TTX and STX binding to wild-type and mutant sodium channels

Data were fit to the Langmuir adsorption isotherm as described in Materials and Methods. K_{app} is the apparent K_d, N is the Hill coefficient, and n is the number of oocytes.

	TTX			STX		
	K_{app}	N	n	K_{app}	N	n
	nM			nM		
Wild-type	18.6 ± 0.8	0.96 ± 0.4	5	2.79 ± 0.1	1.04 ± 0.05	5
E909Q	17.0 ± 1.3	ND[a]	3	2.79 ± 0.39	ND	3
D917N	20.8 ± 2.4	ND	3	2.70 ± 0.22	ND	3
E919Q	19.4 ± 1.4	ND	4	3.25 ± 0.13	ND	3
D927N	18.7 ± 0.5	1.01 ± 0.08	5	2.78 ± 0.16	1.00 ± 0.04	5
E942Q	32,650 ± 7,450	0.93 ± 0.03	4	4,840 ± 550	1.24 ± 0.13	3
E945Q	5,440 ± 770	1.07 ± 0.12	3	54,060 ± 13,200	ND	3
D949N	46.4 ± 4.3	1.03 ± 0.05	3	8.83 ± 0.19	1.06 ± 0	3
E952Q	19.3 ± 0.4	ND	3	4.05 ± 0.92	ND	3

[a] ND, not determined.

30). Although the mechanism for calcium block is unknown, one hypothesis is that it may result from the binding of calcium ions to negative charges within the pore region of the channel, thus blocking passage of sodium ions. We therefore tested whether any of the charge-neutralization mutations affected calcium block, by comparing peak current amplitudes in the presence of 1.8 mM external calcium and 0.18 mM external calcium. Fig. 7A shows the current-voltage relationship for wild-type sodium channels. The peak current amplitude was slightly larger with 0.18 mM external calcium, compared with that in the presence of 1.8 mM calcium. In addition, there was a slight negative shift in the peak of the current-voltage relationship. On average, the peak current amplitude was 1.15 times as large in the presence of 0.18 mM calcium for the wild-type channel (Table 4). All of the mutant sodium channels also demonstrated larger peak current amplitudes in the presence of 0.18 mM calcium, with ratios ranging from 1.10 to 1.42 (Table 4). All of the mutant sodium channels also exhibited a comparable negative shift in the peak of the current-voltage relationship (data not shown). Therefore, none of the negative charges in the domain II S5-S6 region is critical for calcium block of the sodium channel.

Sodium channels are also blocked by protons, probably by their binding to an acidic group with a pK_a of 5.2–5.4 (22). It was possible that one or more of the negatively charged amino acids in the domain II S5-S6 region could be part of the site for proton binding. We therefore examined proton block of the sodium channels expressed in oocytes by comparing the peak current amplitudes measured in an external solution of ND96 at pH 7.5 with the peak current amplitudes obtained in an external solution of ND96 at pH 6.0. Peak current amplitudes were converted to peak conductance values as described in Materials and Methods. Fig. 7B shows that the conductance for wild-type sodium channels at pH 6.0 was decreased, relative to the conductance at pH 7.5, at all potentials. The data were fitted to a theoretical model that describes block by protons at an acidic site within the membrane electric field (22). The model allows the estimation of the pK_a of the putative binding site, taking into account the shift in voltage dependence of activation. The pK_a values ranged from 5.5 to 5.9 (Table 4), in close agreement with the results of Woodhull (22). The pK_a values for all of the mutants were comparable to that of the wild-type sodium channel, suggesting that none of these negative charges is directly involved in proton block of sodium channels.

Discussion

In this report we have examined the functional importance of the eight acidic amino acid residues in the proposed pore-forming region of domain II of the sodium channel (domain II S5-S6) by constructing mutations that individually neutralize each of the negative charges. Despite the fact that all of these mutations affect the charge in this region, none of them had any significant effects on the voltage dependence of either peak conductance or inactivation (Fig. 1 and Table 1). These results suggest that these charges do not interact to any substantial extent with the voltage sensors of the channel, nor do they have any major effect on the overall conformation of the channel. For these reasons we are assuming that the functional effects of these mutations are likely to be localized.

To assess the role of these charges in ion permeation we have examined the effects of the mutations on the inhibition of channel function by TTX and STX, two toxins that are known to bind near the external mouth of the pore (2). Our results indicate that there are three negative charges in domain II S5-S6 that contribute to the binding affinity of the channel for TTX and STX, i.e., E942Q, E945Q, and D949N (Fig. 2 and Table 2). Mutations E942Q and E945Q have already been reported by Terlau *et al.* (19), and our results are consistent with their data. Mutation D949N reduced the affinity for TTX by only 2.5-fold and that for STX by 3.2-fold. The small changes in K_{app} suggested that the aspartate at position 949 might be interacting with TTX electrostatically through space, as has been shown for some of the acidic residues in the *Shaker* potassium channel (10). However, decreasing the ionic strength by approximately half had a similar effect on TTX block of both the wild-type and D949N mutant channels, suggesting that this residue probably does not interact with TTX solely by an electrostatic through-space mechanism. Because the effect of the mutation was small, however, we may have been unable to detect an effect of ionic strength. This could be tested more rigorously by substituting other amino acids with differing charges at that site to see whether the effects are consistent with charge.

Although Terlau *et al.* (19) previously reported that neutralization of the glutamate at position 942 or that at position 945 reduces sensitivity of the sodium channel to TTX and STX, they presented only lower limits for the K_{app} values for TTX of all but E945Q. Our results allow a more quantitative comparison of the effects of these mutations on the binding energies for both toxins. Neutralization of the charge at position 942

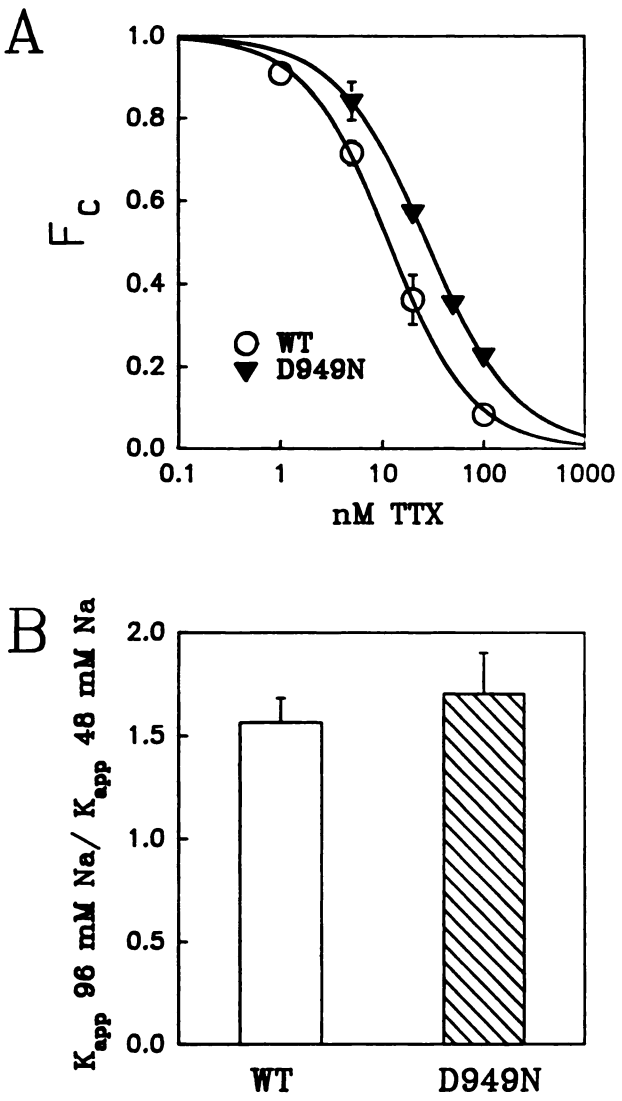

Fig. 4. TTX dose response at low ionic strength. Oocytes expressing the wild-type (*WT*) or D949N mutant sodium channels were perfused with ND96 containing 48 mM NaCl and 48 mM sucrose, and peak sodium currents were measured at test potentials known to elicit the maximum inward current (between 0 and −5 mV). Peak currents were again measured after perfusion of the the recording chamber with at least 10 bath volumes of ND96 containing varying concentrations of TTX. To avoid use-dependent block, pulses were no more frequent than 90 sec apart. The oocytes were then perfused with ND96 to allow measurement of the peak current after the toxins had been washed out. A, *Data points* represent the means of at least three separate determinations, and the *error bars* are standard deviations. The *curves* were generated by a best fit to a Langmuir isotherm, as described in Materials and Methods. The K_{app} values were calculated by best fits to the data and are 11.5 ± 0.9 nM for the wild-type channel and 27.3 ± 3.0 nM for D949N. B, The ratio of the K_{app} at 96 mM NaCl to the K_{app} at 48 mM NaCl was calculated for both the wild-type channel (1.6 ± 0.1) and the D949N mutant (1.7 ± 0.2). The *bars* represent the means of three determinations, and the *error bars* represent 1 SD.

had essentially the same effect on binding of both TTX (1760-fold) and STX (1730-fold), suggesting that this residue may interact in a similar manner with both toxins. This is equivalent to a change in the binding energy of about 4.4 kcal for both toxins. On the other hand, neutralization of the charge at position 945 dramatically decreased the affinity for STX (19,380-fold) but had a lesser effect on the affinity for TTX

TABLE 3

TTX block of sodium channels at −60 mV and −100 mV holding potential

The affinity of wild-type and mutant sodium channels for TTX was assayed at a holding potential of −60 mV. Oocytes were held at −60 mV for at least 10 min in ND96 to allow recovery from slow inactivation and stabilization of the peak current. Oocytes were then perfused with at least 5 ml of ND96 containing TTX at concentrations near that required for 30% block at −100 mV. After stabilization, the peak currents were measured. Test pulses were given every 2 min (or longer) to avoid artifacts due to slow recovery from inactivation and use dependence. TTX was washed off by perfusion with ND96, and the peak currents were again measured. Apparent K_d values were calculated using the equation $K_{app} = [TTX] \cdot [F_c/(1 - F_c)]$, where [TTX] is the concentration of TTX and F_c is the fraction of maximum current remaining after block by TTX.

	K_{app}		Ratio (K_{app} at −100 mV)/ (K_{app} at −60 mV)
	−100 mV	−60 mV	
Wild-type	18.6 ± 0.8 nM	7.0 ± 0.9 nM	2.7
E909Q	17.0 ± 1.3 nM	6.7 ± 0.7 nM	2.5
D917N	20.8 ± 2.4 nM	8.1 ± 0.9 nM	2.6
E919Q	19.4 ± 1.4 nM	5.9 ± 0.7 nM	3.3
D927N	18.7 ± 0.5 nM	9.7 ± 3.3 nM	1.9
E942Q	32.7 ± 7.5 μM	3.3 ± 1.1 μM	9.9
E945Q	5.4 ± 0.8 μM	0.5 ± 0.1 μM	11.3
D949N	46.4 ± 4.3 nM	18.6 ± 5.5 nM	2.5
E952Q	19.3 ± 0.4 nM	8.5 ± 1.1 nM	2.3

(290-fold). These are equivalent to binding energy changes of 5.8 kcal and 3.4 kcal, respectively. Therefore, the glutamate at position 945 has a stronger interaction with STX than with TTX, even though it is only three amino acids away from position 942. Given the different structures of TTX and STX, it is not surprising to observe these differential effects. Terlau *et al.* (19) noted similar, although less dramatic, effects of amino acid substitutions in other domains of the sodium channel.

Because amino acids 942 and 945 and the comparable residues in the other three domains appear to be critical for the binding of TTX and STX, it seems likely that these regions of the molecule are at the external mouth of the pore. The aspartate at position 949 probably lies on the external surface slightly removed from the pore, because neutralization of this residue had only a slight effect on TTX and STX binding. If these conclusions are correct, then the part of the channel that traverses the membrane as the pore must lie to the amino-terminal side of amino acid 942, in the region called SS1 by Guy and Conti (16). Because mutation of the aspartate at position 927 does not affect toxin binding, this residue neither contributes to the structure of the pore nor interacts with the toxins. D927N has a single-channel conductance similar to that of the wild-type channel,[1] so that the negative charge at this position also is not critical for sodium conduction. The fact that none of the other mutations, including E919Q and D917N, affected toxin binding indicates that these residues also are not on the external surface of the channel or that they are located too far from the toxin binding site to have a significant electrostatic interaction with the toxins. If the latter alternative is the case, then it implies that the toxins interact with a very small region in the amino-terminal end of the S5-S6 segment of domain II.

Sodium channels interact with both TTX and STX in a use-dependent manner. One model for this use-dependent block is that the toxins can interact with the sodium channel in at least two slightly different ways, resulting in a low affinity state observed at −100 mV holding potential and a high affinity state

[1] K. J. Kontis and A. L. Goldin, unpublished observations.

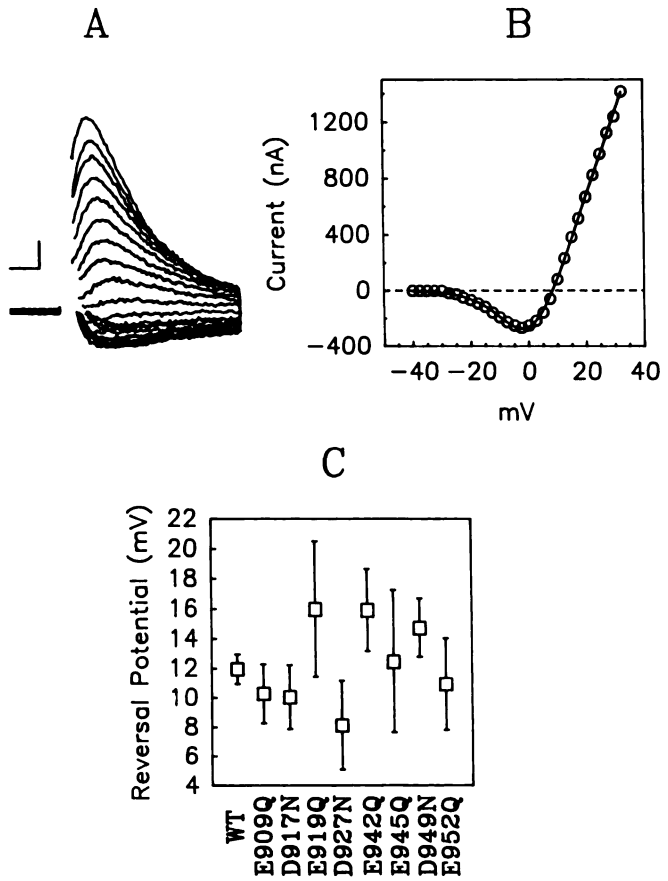

Fig. 5. Determination of reversal potential in the presence of guanidine. Oocytes expressing wild-type (*WT*) sodium channels were perfused with a bathing solution containing 96 mM guanidinium as the permeant ion, and currents were measured during 12-msec test pulses from −40 to +32.5 mV in 2.5-mV steps. Whole-cell currents in ND96 were 5–50 μA. Results from one oocyte are shown. A, Current traces elicited by test pulses from −17.5 to 32.5 mV. *Vertical bar*, 200 nA; *horizontal bar*, 2 msec. B, Current-voltage relationship from the data in A. The *smooth line* is a best fit of the data to a two-state Boltzmann function, as described in Materials and Methods. C, Guanidinium reversal potentials were calculated using the best fit of the data as described in B. *Data points* represent the means of at least three separate determinations, and the *error bars* are standard deviations.

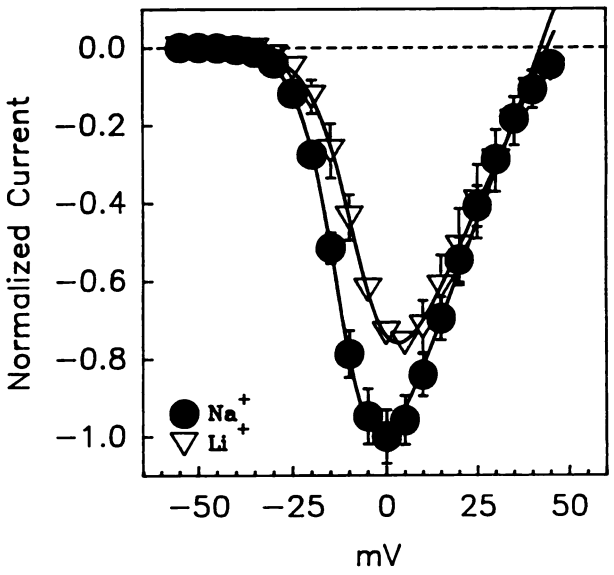

Fig. 6. Measurement of lithium currents through sodium channels. Oocytes expressing wild-type sodium channels were used to record sodium and lithium currents during a series of 12-msec test pulses from −90 to +55 mV in 5-mV increments, using first 96 mM NaCl and then 96 mM LiCl in the bathing solution. Currents were then measured again after washout with ND96. The current-voltage relationship shows data obtained from three oocytes injected with wild-type RNA. ●, Average sodium current before and after application of lithium; ▽, lithium currents. The *error bars* are 1 SD. The *curves* are best fits to the Boltzmann function described in Materials and Methods. Block by lithium was determined by dividing the peak lithium current by the average peak sodium current for each oocyte. The average block by lithium for wild-type and mutant sodium channels is shown in Table 4.

TABLE 4

Ionic block of sodium channels

Peak inward currents were measured using three test solutions, (i) ND96 that had 96 mM Li^+ substituted for Na^+, (ii) ND96 with 0.18 mM Ca^{2+}, and (iii) ND96 at a pH of 6.0. Peak currents were also measured using ND96 as the recording bath solution before and after application of test solutions. For lithium and calcium, block was calculated by dividing peak current in the presence of test solutions by the average peak current in normal ND96. For proton block, pK_a was determined according to the model developed by Woodhull (22), as described in Materials and Methods. In all three cases the values represent means ± standard deviations for at least three determinations each.

	I_{Li^+}/I_{Na^+}	$I_{0.18\ mM\ Ca^{2+}}/I_{1.8\ mM\ Ca^{2+}}$	pK_a
Wild-type	0.75 ± 0.06	1.15 ± 0.15	5.9 ± 0.1
E909Q	0.81 ± 0.05	1.26 ± 0.45	5.8 ± 0.2
D917N	0.81 ± 0.08	1.25 ± 0.31	5.9 ± 0.3
E919Q	0.77 ± 0.06	1.42 ± 0.13	5.9 ± 0.4
D927N	0.76 ± 0.05	1.37 ± 0.04	5.6 ± 0.1
E942Q	0.86 ± 0.04	1.10 ± 0.13	5.5 ± 0.1
E945Q	0.85 ± 0.04	1.20 ± 0.05	5.7 ± 0.1
D949N	0.82 ± 0.09	1.37 ± 0.21	5.6 ± 0.1
E952Q	0.76 ± 0.05	1.34 ± 0.06	5.7 ± 0.1

observed at the more depolarized holding potential of −60 mV (9). The wild-type channel demonstrated a 2.7-fold increase in affinity at −60 mV, compared with −100 mV (Table 3). Of the mutants that we examined, the five that did not affect TTX block at −100 mV also did not affect block at −60 mV. In addition, the D949N mutation changed the sensitivity to TTX to an equivalent extent at both potentials. However, the two mutants that were highly resistant to TTX demonstrated more of a change in sensitivity at −60 mV, compared with −100 mV. Mutant E942Q had a ratio of K_{app} at −100 mV to that at −60 mV of 9.9, and E945Q had a ratio of 11.3. These results indicate that the negative charges at both of these sites make a greater contribution to the binding of TTX when the channel is in the low affinity state (−100 mV) than when the channel is in the high affinity state (−60 mV). It is possible that the two different affinity states of the channel reflect binding of the toxins to completely different sites. If this is the case, however, then the effect of holding potential on toxin binding indicates that the binding is also specific in the low affinity state of the channel.

The guanidinium selectivity of the wild-type sodium channel was apparently not altered by neutralization of negative charges within domain II S5-S6 (Fig. 6), even for those mutants that were highly resistant to the guanidinium toxins TTX and STX. It is likely that the inward guanidinium currents through mutant channels E942Q and E945Q are reduced, as is the case for inward sodium currents. However, this must be examined by more refined methods such as patch clamping or fluctuation analysis (19). The fact that TTX-resistant mutants have wild-type reversal potentials for guanidinium suggests that the glutamates at positions 942 and 945 do not affect permeability. This is consistent with the idea that these residues, and the

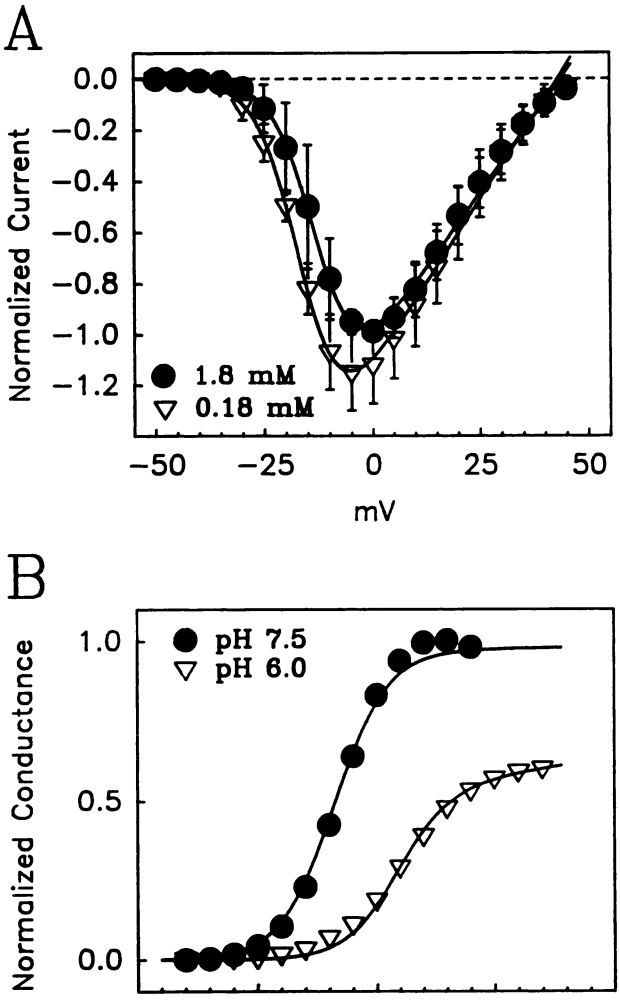

Fig. 7. Block of sodium channels by protons or calcium. A, Peak currents were measured while oocytes expressing wild-type sodium channels were perfused with ND96 containing 1.8 mM $CaCl_2$ and then with ND96 containing 0.18 mM $CaCl_2$. Currents were normalized to the peak current in ND96, and the normalized current-voltage relationships are shown. The *smooth curves* are fits to a Boltzmann distribution, as described in Materials and Methods. B, Peak currents were measured while oocytes were perfused with ND96 at pH 7.5 and then with ND96 at pH 6.0. Normalized conductance values were calculated as described in Materials and Methods. The *smooth curves* are best fits to a mathematical model describing proton block, as described in Materials and Methods. For the experiments in both A and B, peak current amplitudes were also measured after the test solutions were washed out with ND96, to correct for current rundown.

corresponding ones in the other three domains, are part of a "prefilter" and act to electrostatically "focus" TTX as it approaches its binding site (10).

None of the mutations had any apparent effect on the relative permeability to lithium ions or on the apparent ability of lithium ions to block the channel. These results suggest that the negative charges in domain II S5-S6 are not critical for selectivity, although it is possible that the charges in one or more of the other three domains may be important for selectivity. Evidence that selectivity is influenced by residues in domains III and IV was obtained by Heinemann *et al.* (20), who found that substitution of a negative charge for either lysine-1422 in domain III or alanine-1714 in domain IV altered the ion selectivity to resemble that of calcium channels. These two residues are located at positions comparable to position 942 in domain II.

All of the mutants were similar to the wild-type sodium channel in their susceptibility to blockade by protons and calcium (Table 4). Proton blockade was shown to be a voltage-dependent process in frog myelinated nerve, indicating that protons bind within the membrane potential. Using the model developed by Woodhull (22), we calculated the apparent dissociation constant of the putative acidic site in the wild-type and mutant channels to be in the range of 5.5 to 5.9. Although E942Q has the lowest pK_a value (5.5), the difference is probably not significant because the standard deviations for many of the mutants are overlapping. The values we obtained are somewhat higher than those obtained by Woodhull (5.2–5.4), most likely because she was able to use data from more positive potentials with the frog node preparation than we were able to use with the two-microelectrode clamp of *Xenopus* oocytes. It is possible that acidic residues in the other three domains contribute to block by cations. Alternatively, uncharged residues may be more important for this property of the channel. Consistent with this idea, Satin *et al.* (31) showed that replacement of a cysteine with tyrosine at position 374 in domain I increased the ability of cadmium ions to block the sodium channel. It may be that block of sodium channels by monovalent and divalent cations is largely due to interactions with uncharged residues.

Acknowledgments

We are grateful to Dr. Jim Hall, Dave Patton, Ray Smith, and Ted Shih for useful discussions during the course of this work and to Bill Conley for excellent technical assistance.

References

1. Catterall, W. A. Neurotoxins that act on voltage-sensitive sodium channels in excitable membranes. *Annu. Rev. Pharmacol. Toxicol.* **20**:15–43 (1980).
2. Kao, C. Y., and S. E. Walker. Active groups of saxitoxin and tetrodotoxin as deduced from actions of saxitoxin analogues on frog muscle and squid axon. *J. Physiol. (Lond.)* **323**:619–637 (1982).
3. Cohen, C. J., B. P. Bean, T. J. Colatsky, and R. W. Tsien. Tetrodotoxin block of sodium channels in rabbit Purkinje fibers. *J. Gen. Physiol.* **78**:383–411 (1981).
4. Clarkson, C. W., T. Matsubara, and L. M. Hondeghem. Evidence for voltage-dependent block of cardiac sodium channels by tetrodotoxin. *J. Mol. Cell. Cardiol.* **20**:1119–1131 (1988).
5. Eickhorn, R., J. Weirich, D. Hornung, and H. Antoni. Use dependence of sodium current inhibition by tetrodotoxin in rat cardiac muscle: influence of channel state. *Pfluegers Arch.* **416**:398–405 (1990).
6. Gonoi, T., S. J. Sherman, and W. A. Catterall. Voltage clamp analysis of tetrodotoxin-sensitive and -insensitive sodium channels in rat muscle cells developing *in vitro*. *J. Neurosci.* **5**:2559–2564 (1985).
7. Salgado, V. L., J. Z. Yeh, and T. Narahashi. Use- and voltage-dependent block of the sodium channel by saxitoxin. *Ann. N. Y. Acad. Sci.* **479**:84–95 (1986).
8. Lonnendonker, U. Use-dependent block of sodium channel in frog myelinated nerve by tetrodotoxin and saxitoxin at negative holding potentials. *Biochim. Biophys. Acta* **985**:153–160 (1989).
9. Patton, D. E., and A. L. Goldin. A voltage-dependent gating transition induces use-dependent block by tetrodotoxin of rat IIA sodium channels expressed in *Xenopus* oocytes. *Neuron* **7**:637–647 (1991).
10. MacKinnon, R., and C. Miller. Mutant potassium channels with altered binding of charybdotoxin, a pore-blocking inhibitor. *Science (Washington D. C.)* **245**:1382–1385 (1989).
11. MacKinnon, R., L. Heginbotham, and T. Abramson. Mapping the receptor site for a pore-blocking potassium channel inhibitor. *Neuron* **5**:767–771 (1990).
12. MacKinnon, R., and G. Yellen. Mutations affecting TEA blockade and ion permeation in voltage-activated K^+ channels. *Science (Washington D. C.)* **250**:276–279 (1990).
13. Yellen, G., M. E. Jurman, T. Abramson, and R. MacKinnon. Mutations affecting internal TEA blockade identify the probable pore-forming region of a K^+ channel. *Science (Washington D. C.)* **251**:939–942 (1991).
14. Hartmann, H. A., G. E. Kirsch, J. A. Drewe, M. Taglialatela, R. H. Joho, and A. M. Brown. Exchange of conduction pathways between two related K^+ channels. *Science (Washington D. C.)* **251**:942–944 (1991).

15. Yool, A. J., and T. L. Schwarz. Alteration of ionic selectivity of a K^+ channel by mutation of the H5 region. *Nature (Lond.)* **349**:700–704 (1991).
16. Guy, H. R., and F. Conti. Pursuing the structure and function of voltage-gated channels. *Trends Neurosci.* **13**:201–206 (1990).
17. Durell, S. R., and H. R. Guy. Atomic scale structure and functional models of voltage-gated potassium channels. *Biophys. J.* **62**:238–250 (1992).
18. Noda, M., H. Suzuki, S. Numa, and W. Stuhmer. A single point mutation confers tetrodotoxin and saxitoxin insensitivity on the sodium channel II. *FEBS Lett.* **259**:213–216 (1989).
19. Terlau, H., S. H. Heinemann, W. Stuhmer, M. Pusch, F. Conti, K. Imoto, and S. Numa. Mapping the site of block by tetrodotoxin and saxitoxin of sodium channel II. *FEBS Lett.* **293**:93–96 (1991).
20. Heinemann, S. H., H. Terlau, W. Stuhmer, K. Imoto, and S. Numa. Calcium channel characteristics conferred on the sodium channel by single mutations. *Nature (Lond.)* **356**:441–443 (1992).
21. Sigworth, F. J., and B. C. Spalding. Chemical modification reduces the conductance of sodium channels in nerve. *Nature (Lond.)* **283**:293–295 (1980).
22. Woodhull, A. M. Ionic blockage of sodium channels in nerve. *J. Gen. Physiol.* **61**:687–708 (1973).
23. Auld, V. J., A. L. Goldin, D. S. Krafte, J. Marshall, J. M. Dunn, W. A. Catterall, H. A. Lester, N. Davidson, and R. J. Dunn. A rat brain Na^+ channel *alpha* subunit with novel gating properties. *Neuron* **1**:449–461 (1988).
24. Kunkel, T. A. Rapid and efficient site-specific mutagenesis without phenotypic selection. *Proc. Natl. Acad. Sci. USA* **82**:488–492 (1985).
25. Krafte, D. S., T. P. Snutch, J. P. Leonard, N. Davidson, and H. A. Lester. Evidence for the involvement of more than one mRNA species in controlling the inactivation process of rat brain Na channels expressed in *Xenopus* oocytes. *J. Neurosci.* **8**:2859–2868 (1988).
26. Kegel, D. R., B. D. Wolf, R. E. Sheridan, and H. A. Lester. Software for electrophysiological experiments with a personal computer. *J. Neurosci. Methods* **12**:317–330 (1985).
27. Saimi, Y., and K.-Y. Ling. Calmodulin activation of calcium-dependent sodium channels in excised membrane patches of *Paramecium*. *Science (Washington D. C.)* **249**:1441–1444 (1990).
28. Hinshaw, J. E., B. O. Carragher, and R. A. Milligan. Architecture and design of the nuclear pore complex. *Cell* **69**:1133–1141 (1992).
29. Hille, B. The permeability of the sodium channel to metal cations in myelinated nerve. *J. Gen. Physiol.* **59**:637–658 (1972).
30. Yamamoto, D., J. Z. Yeh, and T. Narahashi. Voltage-dependent calcium block of normal and tetramethrin-modified single sodium channels. *Biophys. J.* **45**:337–344 (1984).
31. Satin, J., J. W. Kyle, M. Chen, P. Bell, L. L. Cribbs, H. A. Fozzard, and R. B. Rogart. A mutant of TTX-resistant cardiac sodium channels with TTX-sensitive properties. *Science (Washington D. C.)* **256**:1202–1205 (1992).

Send reprint requests to: Dr. Alan L. Goldin, Department of Microbiology and Molecular Genetics, University of California, Irvine, CA 92717.